

Optical properties of ZnCr_2Se_4 : spin-phonon coupling and electronic d-d-like excitations

T. Rudolf, Christian Kant, Franz Mayr, M. Schmidt, Vladimir Tsurkan, Joachim Deisenhofer, Alois Loidl

Angaben zur Veröffentlichung / Publication details:

Rudolf, T., Christian Kant, Franz Mayr, M. Schmidt, Vladimir Tsurkan, Joachim Deisenhofer, and Alois Loidl. 2009. "Optical properties of ZnCr_2Se_4 : spin-phonon coupling and electronic d-d-like excitations." *The European Physical Journal B* 68 (2): 153–60.
<https://doi.org/10.1140/epjb/e2009-00096-4>.



Optical properties of ZnCr_2Se_4

Spin-phonon coupling and electronic d-d-like excitations

T. Rudolf^{1,a}, Ch. Kant¹, F. Mayr¹, M. Schmidt¹, V. Tsurkan^{1,2}, J. Deisenhofer¹, and A. Loidl¹

¹ Experimental Physics V, Center for Electronic Correlations and Magnetism, University of Augsburg, 86135 Augsburg, Germany

² Institute of Applied Physics, Academy of Sciences of Moldova, MD-2028 Chişinău, Republic of Moldova

Abstract. We studied the optical properties of antiferromagnetic ZnCr_2Se_4 by infrared spectroscopy up to $28,000\text{ cm}^{-1}$ and for temperatures from 5 to 295 K. At the magnetic phase transition at 21 K, one of the four phonon modes reveals a clear splitting of 3 cm^{-1} as a result of spin-phonon coupling, the other three optical eigenmodes only show shifts of the eigenfrequencies. The antiferromagnetic ordering and the concomitant splitting of the phonon mode can be suppressed in a magnetic field of 7 T. At higher energies we observed a broad excitation band which is dominated by a two-peak-structure at about $18,000\text{ cm}^{-1}$ and $22,000\text{ cm}^{-1}$, respectively. These energies are in good agreement with the expected spin-allowed crystal-field transitions of the Cr^{3+} ions. The unexpected strength of these transitions with $d-d$ character is attributed to a considerable hybridization of the selenium p with the chromium d orbitals.

PACS. 63.20.-e Phonons in crystal lattices – 75.50.Ee Antiferromagnetics – 78.30.-j Infrared and Raman spectra

1 Introduction

The B -site magnetic ions in the normal spinels AB_2X_4 form a corner sharing tetrahedral network, the well known pyrochlore lattice, which is strongly frustrated. Specifically in Cr spinels geometrical frustration and bond frustration compete and produce a complex phase diagram as function of lattice constant or Curie-Weiss (CW) temperature [1]. The oxides with the smallest lattice constants are dominated by direct antiferromagnetic (AFM) exchange between neighboring Cr ions and hence are strongly geometrically frustrated. With increase of the Cr-Cr separation in the sulfides and selenides, the 90° ferromagnetic (FM) Cr- X -Cr exchange gains increasing importance and finally constitutes a FM ground state in CdCr_2S_4 , CdCr_2Se_4 and HgCr_2Se_4 . Theoretical calculations of these exchange couplings have been recently performed within the Local Spin Density Approximation (LSDA) [2]. The majority of the chromium spinels undergoes AFM order close to 10 K, despite the fact that the CW temperatures range from -400 K to 140 K [1,3]. In the AFM systems the magnetic ordering is accompanied by a structural transition from the cubic normal spinel structure to either tetragonal or orthorhombic symmetry. The origin of this symmetry reduction has been attributed to a spin-driven Jahn-Teller effect [4,5].

In the case of ZnCr_2Se_4 the room temperature cubic symmetry with space group $Fd\bar{3}m$ (7O_h) is lost at $T_N = 21\text{ K}$ and the system was found to become tetragonal with space group $I4_1/amd$ ($^{19}D_{4h}$) [6]. Recently, a minute orthorhombic distortion was reported leading to the assignment of space group $Fddd$ ($^{24}D_{2h}$) [7]. The magnetic susceptibility can be described by a *ferromagnetic* CW temperature of $\Theta_{CW} = 90\text{ K}$ and an effective chromium moment, which is very close to the spin-only value of Cr^{3+} in an octahedral environment ($S = 3/2$) [8]. The spin structure below T_N is characterized by ferromagnetic (001) planes with a turn angle of the spin direction of 42° between neighboring planes [6,7]. There are recent reports on large magnetostriction and on negative thermal expansion [8], as well as on multiferroicity [9,10].

The symmetry reduction at the magnetic phase transition can hardly be detected by conventional X-ray diffraction, but manifests clearly in the lattice dynamics and a splitting of the infrared (IR) active phonon modes below the magnetic ordering temperature has been reported for several AFM spinels [1,11–13]. From these splittings the spin-phonon coupling was deduced in some cases [12,13]. Notably, the magnetic transition in ZnCr_2Se_4 can be fully suppressed in external magnetic fields of 6.5 T [8] and the splitting of the optical phonons disappears as cubic symmetry is restored [14].

^a e-mail: torsten.rudolf@physik.uni-augsburg.de

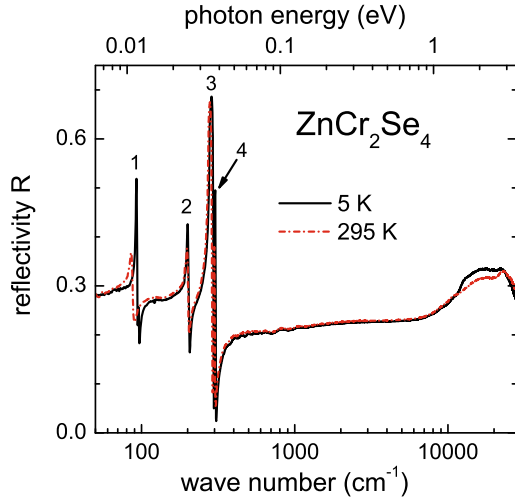


Fig. 1. (Color online) Reflectivity vs. wave number for ZnCr_2Se_4 at 5 K (solid line) and 295 K (dash-dotted line).

This paper is intended as a detailed and comprehensive analysis of the IR experiments in ZnCr_2Se_4 across the magneto-structural transition and in the presence of an external magnetic field, which was partly described in a previous brief publication [14]. Moreover, we performed reflectivity measurements up to $28,000 \text{ cm}^{-1}$, where electronic transitions could be observed, which bear the energy scales of local $d-d$ excitations within the crystal-field d multiplet.

2 Experimental details

Single crystals with $a = 1.0498(2) \text{ nm}$ and a selenium fractional coordinate of $x = 0.260$, which were characterized in earlier investigations [8,14], have been used for the optical experiments. The reflectivity measurements were carried out in the frequency range from 50 to $28,000 \text{ cm}^{-1}$ using the Bruker Fourier-transform spectrometers IFS 113v and IFS 66v/S, which both are equipped with He bath cryostats. For the phonon evaluation we analyzed the measured reflectivity directly utilizing a standard Lorentz model for the complex dielectric function

$$\epsilon(\omega) = \epsilon_\infty + \sum_j \frac{\Delta\epsilon \cdot \omega_{TO,j}^2}{\omega_{TO,j}^2 - \omega^2 - i\gamma_j\omega}, \quad (1)$$

with the program RefFIT developed by A. Kuzmenko [15]. For each phonon mode j , the fit parameters are the transverse optical eigenfrequency $\omega_{TO,j}$, the dielectric strength $\Delta\epsilon$ and the damping $\gamma_{TO,j}$. The parameter ϵ_∞ results from electronic polarizabilities only and has been determined from fits up to $5,000 \text{ cm}^{-1}$ before the onset of the electronic transitions (see Fig. 1). We found that $\epsilon_\infty = 8.0(1)$ at room temperature and smoothly decreases to values close to $7.8(1)$ at the lowest temperatures. To calculate the dielectric loss function or the real part of the optical conductivity from the reflectivity we used the Kramers-Kronig relation with a constant extrapolation towards low frequencies and a smooth $\omega^{-1.6}$ extrapolation to high frequencies.

3 Experimental results and discussion

Figure 1 shows the reflectivity R of ZnCr_2Se_4 as measured on single crystalline samples at room temperature (295 K: red dash-dotted line) and at 5 K (black solid line) for wave numbers ranging from 50 up to $28,000 \text{ cm}^{-1}$. At frequencies below 400 cm^{-1} four phonons are detected. The excitations 3 and 4 at approximately 300 cm^{-1} are very close in energy and can be distinguished more easily in Figure 2. The reflectivity in the phonon regime is followed by a flat and structureless plateau up to $7,000 \text{ cm}^{-1}$ and a subsequent increase due to electronic excitations. Both, the phonons and the electronic excitations, are obviously temperature dependent and will be discussed separately in the following.

3.1 Phonon excitations

Figure 2 shows the dielectric loss ϵ'' of ZnCr_2Se_4 in the phonon regime below 400 cm^{-1} , at room temperature and at 5 K, well below the Néel temperature ($T_N = 21 \text{ K}$). At 295 K four modes located approximately at 85, 200, 275 and 300 cm^{-1} can be identified, corresponding to the four triply-degenerate IR-active $T_{1u}(j)$ modes ($j = 1, 2, 3, 4$) expected from a normal mode analysis [16]:

$$\begin{aligned} \Gamma &= 4T_{1u} && \text{(IR active)} \\ &+ A_{1g} + E_{1g} + 3T_{2g} && \text{(Raman active)} \\ &+ 2A_{2u} + 2E_u + T_{1g} + 2T_{2u} && \text{(silent)} \end{aligned}$$

Upon cooling shifts in the eigenfrequencies are detected. When entering the magnetically ordered regime at T_N mode $T_{1u}(1)$ reveals a clear splitting into two modes (see inset of Fig. 2).

The detailed temperature dependence of the transversal eigenfrequencies and the corresponding damping constants are shown in the first two columns of Figure 3, with-

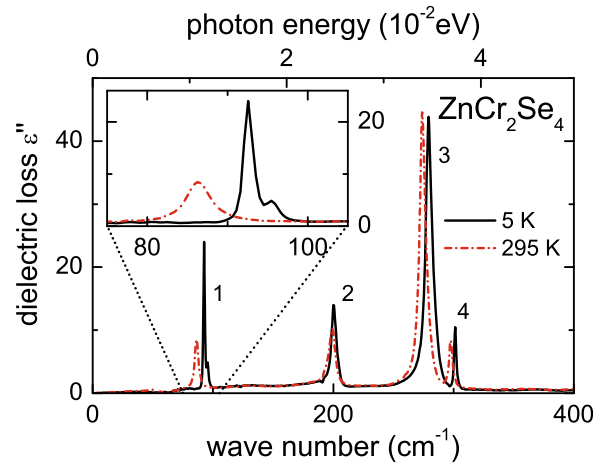


Fig. 2. (Color online) Dielectric loss vs. wave number of ZnCr_2Se_4 for 5 K (solid line) and 295 K (dash-dotted line). The inset shows an enlarged region around 90 cm^{-1} to document the phonon splitting at low temperatures.

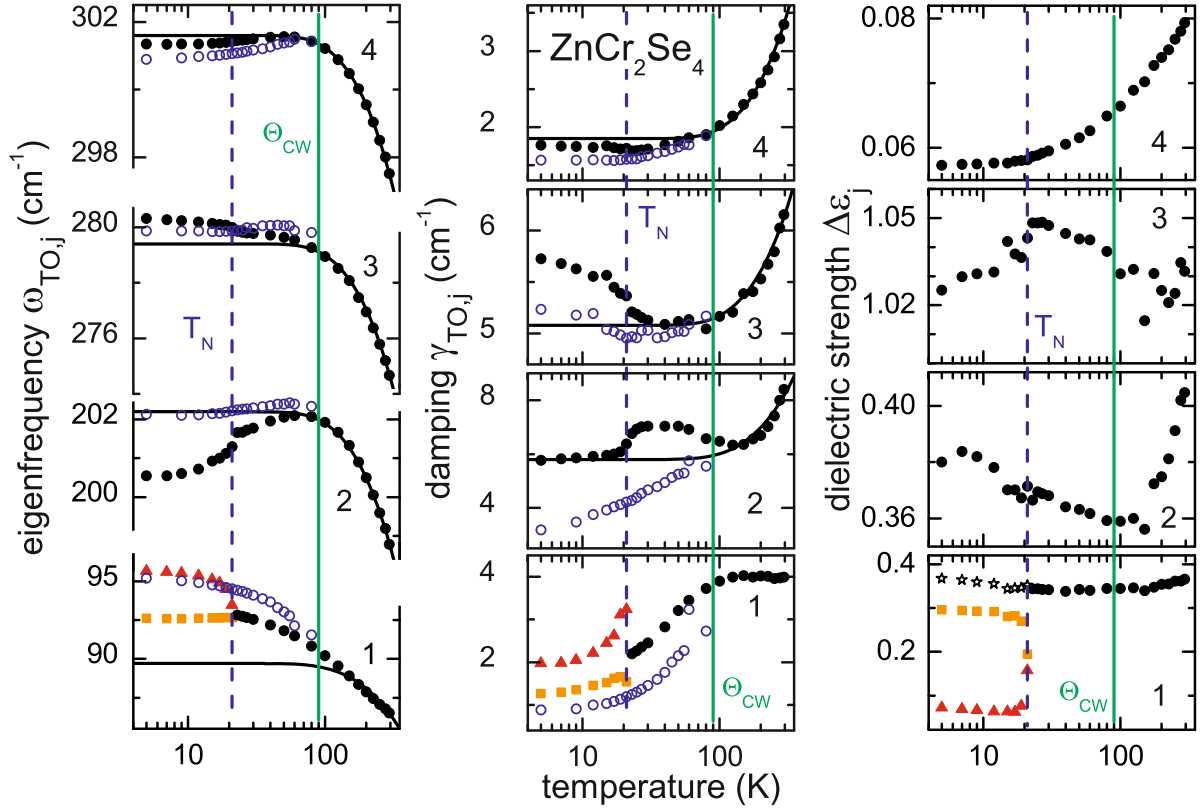


Fig. 3. Eigenfrequencies (left frame), damping constants (middle frame) and dielectric strengths (right frame) of ZnCr_2Se_4 vs. temperature for all eigenmodes on semilogarithmic scales. The antiferromagnetic ordering temperature and the Curie-Weiss temperature are indicated. Closed symbols: $H = 0$ T, open circles: $H = 7$ T.

out magnetic field and in a field of 7 T. In the third column we show the temperature dependence of the dielectric strength. The relevant magnetic temperature scales given by $T_N = 21$ K and the ferromagnetic CW temperature $\Theta_{CW} = 90$ K are indicated to reveal a possible influence of ferromagnetic fluctuations and magnetic ordering on the phonon properties.

Starting with the temperature dependence of the transversal eigenfrequencies in the left frame of Figure 3, one can see that the shift is dominated by canonical anharmonic effects for $T > 100$ K (black solid lines), i.e. it originates from phonon-phonon interactions: all phonon modes harden on decreasing temperature. To get an estimate of the anharmonic effect, we followed a simple approach, outlined in reference [17], where only a prefactor and an average Debye temperature enter into the fit of the high-temperature data. The Debye temperature was calculated from the IR active phonon modes and was kept constant at $\Theta_D = 308$ K for all fits shown in Figure 3. However, below the temperature scale of $\Theta_{CW} = 90$ K this continuous increase is interrupted. Mode 2 and 4 start to decrease, while modes 1 and 3 increase even stronger than the purely anharmonic processes suggest. Evidently, mode 4 does not change at $T_N = 21$ K, mode 1 splits, and mode 2 and 3 show a shift that might be considered to

mimic the behavior of magnetic sublattice-order parameters.

Early on, K. Wakamura proposed a phenomenological model of how AFM and FM exchange interactions lead to a positive or negative shift of the phonon eigenfrequencies [18], but both experimental and theoretical work has shown that the coupling between lattice dynamics and exchange couplings is more intricate [1,19]. Furthermore, the significant differences in the temperature dependence of the damping constants of the respective phonon modes can not easily be explained along existing models [20].

To sort out the influence of AFM interactions on each mode, we look at the temperature dependence of the modes in an applied magnetic field of 7 T. At this field the AFM transition is suppressed and the system remains cubic. It becomes clear that $T_{1u}(4)$ does not change significantly upon the suppression of AFM fluctuations and is already dominated by FM interactions in zero field. Note that also the damping constant of this mode is well described by anharmonic effects (black solid line) in the whole temperature range. The dielectric strength decreases towards lower temperatures without any anomalies at Θ_{CW} or T_N .

The positive shift of $T_{1u}(3)$ in zero magnetic field and below T_N seems to originate from the AFM ordering only,

Table 1. Table of low temperature structures, observed and expected IR active phonon modes, and the size of the phonon splitting of different Cr spinels ACr_2X_4 .

Compound	Θ_{CW}	T_{N}	space group for $T < T_{\text{N}}$	IR-modes obs. (exp.)	size of splitting in cm^{-1} for the T_{1u} mode (j) and $T < T_{\text{N}}$	new modes at freq. in cm^{-1}	Refs.
ZnCr_2O_4	-398	12.5	$I\bar{4}m2$	5 (15)	11 (2)	553	[26],[12],[1]
ZnCr_2S_4	7.9	15	$I4_1/amd$	5 (10)	4 (3)		[25]
		8	$Imma$	12 (20)	5 (1), 3 (2), 4 (3), 3 (4)	130, 262, 350, 381	[25]
ZnCr_2Se_4	90	21	$I4_1/amd$	5 (10)	3 (1)		[6]
HgCr_2S_4	140	22	$Fd\bar{3}m$	4 (4)	0	-	[25]

as a magnetic field of 7 T leads to a suppression of that slight positive shift. The damping of this mode is well described by anharmonic effects with an additional strong increase below T_{N} which can be suppressed in a magnetic field of 7 T. For decreasing temperatures $\Delta\epsilon$ seems to increase in the range $T_{\text{N}} < T < \Theta_{\text{CW}}$ and decreases below T_{N} .

The order-parameter-like negative shift of mode $T_{1u}(2)$ below T_{N} also disappears in a field of 7 T, relating this shift to the AFM ordering. The damping of this mode is dominated by anharmonicity with an additional contribution appearing only between $T_{\text{N}} < T < \Theta_{\text{CW}}$. In a magnetic field of 7 T the damping of mode 2 continuously decreases towards lower temperatures without any anomalies. The dielectric strength decreases between room temperature and Θ_{CW} and increases towards lower temperatures for $T < \Theta_{\text{CW}}$.

Obviously, the splitting is absent for mode $T_{1u}(1)$ in 7 T and the eigenfrequency continuously increases towards lower temperatures. The damping constants decrease with decreasing temperatures both above and below the magnetic phase transition. The application of 7 T leads to a somewhat smaller damping with a similar temperature dependence as in zero field. $\Delta\epsilon$ of mode 1 and its continuation as a sum of the dielectric strengths of the split modes behaves similar to mode 2. The dielectric strengths of the split modes at 5 K yield a ratio of approximately 1:4.

It is important to note that the behavior in 7 T of all modes except $T_{1u}(2)$ is very similar to the behavior of HgCr_2S_4 which still orders antiferromagnetically but does not show a splitting, and to the ferromagnet CdCr_2S_4 [17]. For $T_{1u}(2)$ the shift in the latter compounds becomes even positive below the magnetic ordering.

Unfortunately, it is not straightforward to single out a simple scheme which relates the competing exchange interactions with the shift and splittings of the normal modes in AFM spinel systems like ZnCr_2Se_4 , since both AFM and FM interactions will be modulated by the lattice dynamics.

Concerning the fact that AFM ordering in these systems is accompanied by a structural symmetry reduction, a splitting of the degenerate cubic $T_{1u}(j)$ modes and the appearance of new modes is expected. Considering that the most common structural distortion for spinels occurring below the Néel temperature is tetragonal with space

group $I4_1/amd$ ($^{19}D_{4h}$) [6,7,21,22] one finds the following normal modes [16]:

$$\begin{aligned}
 \Gamma &= 4A_{2u} + 6E_u && \text{(IR active)} \\
 &+ 2A_{1g} + 3B_{1g} + B_{2g} + 4E_g && \text{(Raman active)} \\
 &+ 2A_{1u} + A_{2g} + 2B_{1u} + 4B_{2u} && \text{(silent)}
 \end{aligned}$$

This corresponds to a splitting of the four cubic T_{1u} and the appearance of two additional E_u modes which are silent in cubic symmetry. The size of the splittings, however, may be beyond the experimental resolution and depend strongly on the competition between FM and AFM interactions.

In Table 1 we compare the number of expected and observed phonon modes for the three AFM spinels ZnCr_2X_4 ($X = \text{O}, \text{S}, \text{Se}$) and for AFM HgCr_2S_4 . These four compounds differ strongly with regard to the competition of AFM and FM exchange couplings. Starting with ZnCr_2Se_4 with a positive CW temperature and strong FM interactions, only the lowest lying phonon splits by 3 cm^{-1} at the magneto-structural transition. The other splittings and the new modes are obviously beyond the resolution. Note that recently a small orthorhombic distortion has been found in ZnCr_2Se_4 , which results in the assignment of space group $Fddd$ ($^{24}D_{2h}$) below T_{N} [7,23]. In this case one would expect to observe 18 IR-active modes [16]. In almost FM HgCr_2S_4 , where AFM order can be suppressed by an external magnetic field well below 1 T [24], not a single phonon mode splits.

In the case of ZnCr_2S_4 , AFM and FM interactions almost compensate each other leading to a relatively low $\Theta_{\text{CW}} = 7.9 \text{ K}$ ($\approx T_{\text{N}}$) and the system undergoes two magneto-structural transitions, first at 15 K to the tetragonal $I4_1/amd$ symmetry and below 8 K to orthorhombic $Imma$ [25]. Interestingly, only mode 3 splits at the first transition, whereas a complete splitting and several new modes are observed in the vicinity of $T_{\text{N}2} = 8 \text{ K}$. The splittings of all T_{1u} modes are of the same order of magnitude.

The system with the strongest antiferromagnetic interaction, ZnCr_2O_4 , reportedly undergoes a different tetragonal distortion with space group $I\bar{4}m2$ [26]. With the assignment of the Wyckoff positions of the atoms still lacking, we assume that in this symmetry Zn, Cr, and O occupy sites with multiplicities of 4, 8, and 16 (similarly to the situation in spinels with tetragonal $I4_1/amd$ symmetry). Then one would expect 15 IR-active phonons.

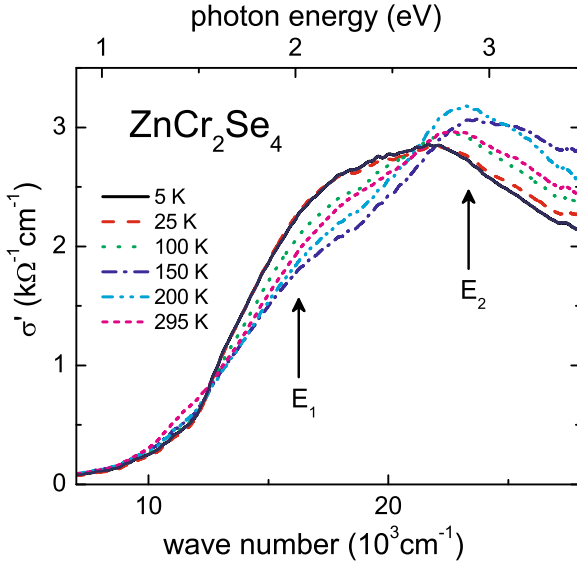


Fig. 4. (Color online) Real part of the conductivity vs. wave number of ZnCr_2Se_4 between 0.9 and 3.5 eV for a series of temperatures. The temperatures are given in the figure, the arrows roughly indicate the energies of the electronic transitions.

Experimentally, however, only a splitting of mode 2 with $\Delta = 11 \text{ cm}^{-1}$ has been observed by A. B. Sushkov and coworkers [12]. Moreover, a small anomaly indicative of a new mode at about 553 cm^{-1} has been reported [1].

Phenomenologically, this comparison suggests that a weak AFM exchange on the background of a strong FM one ($\Theta_{\text{CW}} = 90 \text{ K}$) favors the splitting of mode 1 ($X = \text{Se}$), while a splitting of other modes is suppressed. Note that in HgCr_2S_4 ($\Theta_{\text{CW}} = 140 \text{ K}$) no splitting has been observed at all. When the interactions almost compensate each other more splittings become observable and are of the same order of magnitude ($X = \text{S}$). With the AFM interaction dominating, mode 2 is split significantly and, again, the splitting of the other modes is suppressed. For ZnCr_2O_4 , the splitting of mode 2 was estimated by Fennie and Rabe [19], and it is desirable to perform such calculations throughout the whole phase diagram to reveal the sensitivity of each single mode on the competing exchange interactions.

3.2 Electronic excitations

Now we turn to discuss the high-energy excitations in ZnCr_2Se_4 . To analyze the electronic transitions the reflectivity was converted into a frequency dependent dielectric loss $\epsilon''(\omega)$ and into the real part of the conductivity $\sigma'(\omega) = \epsilon_0 \omega \epsilon''(\omega)$, with the dielectric permittivity of vacuum ϵ_0 . Both quantities reveal a two-peak structure (see below) indicating at least two distinct electronic excitations.

The conductivity (Fig. 4) is dominated by a strong excitation, reaching a maximum of $\approx 3,000 \Omega^{-1}\text{cm}^{-1}$, with an onset at $\approx 10,000 \text{ cm}^{-1}$ and extending up to frequencies $> 28,000 \text{ cm}^{-1}$, beyond our experimentally accessible

frequency range. At room temperature the dielectric loss has been determined from reflectance spectra in the energy range from 4 to 100 eV by S. Suga *et al.* [27]. Their data show a continuous decrease of $\epsilon''(\omega)$ between 4 eV and 20 eV. We would like to point out that similar features are observed in the reflectivity for many chalcogenide spinel systems, e.g. CdCr_2Se_4 [28] and CdCr_2S_4 [29]. Historically, the onset of this two-peak structure has been investigated by absorption measurements, but given the low transmission of these systems only the very onset of these excitation could be detected and its changes with temperature became subject to a controversial discussion about strong and anomalous absorption-edge shifts and the related magnetic derived changes of the band structure in Cr spinels [30–35].

Early on, there have been suggestions that these absorption edges are not due to interband transitions, but correspond to excitonic-like onsite $d-d$ excitations within the band gaps [36–38], while the charge transfer excitations occur only at higher energies. Indeed, the two maxima at 295 K in $\epsilon''(\omega)$ are located at about $18,000 \text{ cm}^{-1}$ and $22,000 \text{ cm}^{-1}$, respectively. These frequencies are in good agreement with typical crystal-field (CF) excitations observed in a large variety of crystals containing trivalent chromium in an octahedral environment [37,39]. To analyze the $d-d$ -like excitations in ZnCr_2Se_4 in a more quantitative way, we investigated the dielectric loss vs. wave number (Fig. 5) by various models. In a first step, we simulated $\epsilon''(\omega)$ with four Gaussian peaks, taking into account also spin-forbidden transitions. In this case, the parameters (eigenfrequency E_j , width and intensity) are highly correlated. Even assuming two spin-allowed transitions with eigenfrequencies E_1 and E_2 results in an almost 100% correlation of width and area of the two peaks. Only constraining the width of the two peaks to be temperature dependent but equal yields reliable fits. A prototypical result is shown in Figure 5(a) for 5 K. The temperature dependence of E_1 and E_2 arising from these fits is shown in Figure 6. The results are very close to those when only the peak maxima are analyzed. As an example we show the dielectric loss spectrum at 295 K [see Fig. 5(b)].

In the crystal-field multiplet scheme for Cr^{3+} these two excitations correspond to the two spin-allowed transitions from the 4A_2 ground state to the 4T_2 and 4T_1 excited states [40]. Neglecting spin-orbit coupling the transition from the ground state to 4T_2 is located just at $10 Dq$, where Dq is the ligand-field coulombic parameter. The Racah parameter B is given by $B = (2E_1 - E_2)(E_2 - E_1)/(27E_1 - 15E_2)$ [37], usually approximated by $(E_2 - E_1)/12$. Hence, the first two excitation energies directly yield the parameters Dq and B . Table 2 lists the values for ZnCr_2Se_4 at 295 K in comparison with other Cr containing spinel systems. Obviously, the two spin allowed CF transitions are approximately at the same energies for different A-site ions and also coincide with the transitions observed in diluted systems like Cr doped ZnAl_2O_4 . The value taken from the literature for ZnCr_2S_4 [41] was derived from absorption and photoconductivity measurements in comparison with CdCr_2S_4 [42]. Reflectivity

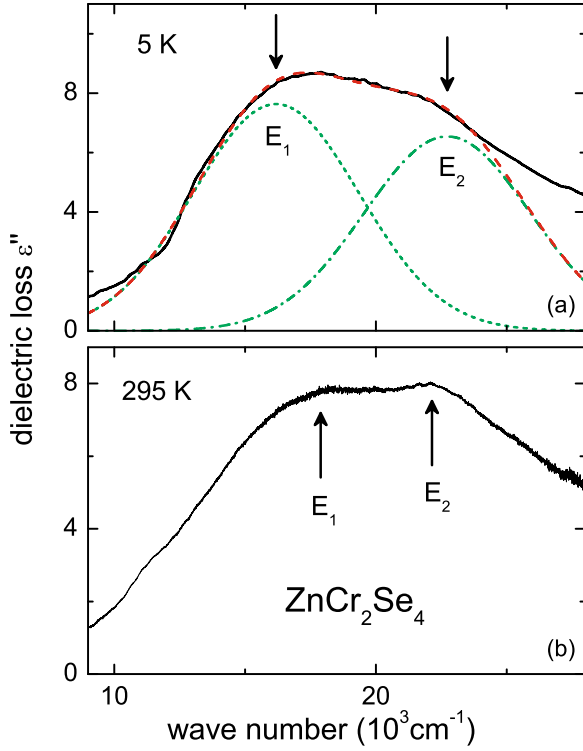


Fig. 5. (Color online) Dielectric loss vs. wave number of ZnCr_2Se_4 at 5 K (upper frame) and 295 K (lower frame). The measurements are indicated by a thick solid line. The fitting results are given by a dashed line. The two peaks, which contribute to the total dielectric loss, are indicated.

Table 2. Electronic $d-d$ transition energies for various spinel systems. The crystal field parameters $10 Dq$ and B are indicated.

Compound	$E_1 = 10Dq$	B	Reference
ZnCr_2Se_4	18041	431	this work
$\text{ZnAl}_2\text{O}_4:\text{Cr}^{3+}$	18756	695	[43]
ZnCr_2O_4	17450	525	[46]
ZnCr_2S_4	14195	220	[41]
CdCr_2S_4	14195	243	[42]
	19900	303	[29]

measurements in CdCr_2S_4 [29] show a similar behavior and excitation energies as in ZnCr_2Se_4 , in contrast to earlier reports. Since the Cr crystal-field levels seem to be unaffected by changes in the lattice constant or the competition of FM and AFM interactions for most of these compounds, it is likely that the assignment of the excitations for ZnCr_2S_4 and CdCr_2S_4 ought to be reconsidered.

The reason for the aforementioned discussion about the onset of the spin allowed CF excitation in terms of an optical band gap is due to the very large oscillator strength of these excitations for the chalcogenides. Usually, local $d-d$ transitions are parity forbidden, but can

e.g. become electric dipole allowed by an admixture of odd phonons (vibronic coupling). The expected oscillator strength in such a case is of the order of $10^{-3} - 10^{-4}$ and one would expect an increase of the oscillator strength and a broadening with temperature [44,45]. Such weak excitations are hardly visible in reflection and, therefore, these transitions are commonly investigated by absorption measurements. For ZnCr_2O_4 strong crystal-field absorption peaks were reported at frequencies of $17,450 \text{ cm}^{-1}$ ($^4A_2 \rightarrow ^4T_2$), $22,700 \text{ cm}^{-1}$ ($^4A_2 \rightarrow ^2T_2$) and $23,850 \text{ cm}^{-1}$ ($^4A_2 \rightarrow ^4T_1$) [46]. In the similar compound CdCr_2O_4 we could not detect any contribution of the CF transitions to the reflectivity [47], while in chalcogenide spinels like ZnCr_2Se_4 the excitations are strong enough to be considered as the optical gap. It is not yet understood how the large oscillator strength can be explained. There is no experimental indication that the parity selection rule is broken on the octahedral B sites, but it could be due to a combined effect of phonon-induced symmetry breaking and strong hybridization of the Cr d -orbitals with the $2p/3p/4p$ of the O/S/Se ligands. This strong hybridization was already derived from photoemission data by M. Taniguchi et al. [48]. A similar tendency was recently reported by K. Ohgushi and coworkers [49] for a variety of oxide and chalcogenide spinel systems. Recent band structure calculations by A. N. Yaresko also favor the assumption of $d-d$ -like transitions as their theoretical energy of 2.7 eV is lying close to our experimental values [2].

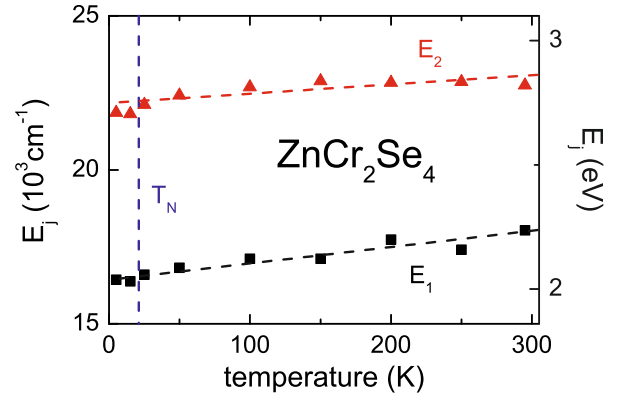


Fig. 6. (Color online) Temperature dependence of the transition energies E_1 and E_2 of ZnCr_2Se_4 as determined from the fits as indicated in Figure 5. The dashed lines are drawn to guide the eye.

The temperature dependence of the two excitations in ZnCr_2Se_4 is shown in Figure 6. These results correspond to fits using two Gaussian peaks of equal width as shown in Figure 5(a). Both excitation energies exhibit only a weak temperature dependence. It is important to note that both excitation energies reveal no significant changes at the AFM ordering temperature. Obviously, the level splitting is only weakly influenced by the magnetic ordering.

4 Summary

We investigated the optical spectrum of ZnCr_2Se_4 across the AFM phase transition at 21 K. The phonon response has been analyzed and discussed in detail as function of temperature and external magnetic field. The temperature dependence of eigenfrequency, damping and dielectric strength of each phonon mode is given. These quantities exhibit a complex pattern, influenced by the onset of FM fluctuations and by AFM order. The results can only partly be explained by existing models [18,20]. The comparison of the observed splittings and the appearance of new modes for the series of ZnCr_2X_4 with $X = \text{O}, \text{S}, \text{Se}$ reveal a complex response of the phonon modes as function of the competing exchange interactions. Moreover, a broad two-peak structure could be observed at higher energies. The excitation energies are in good agreement with chromium onsite crystal-field excitations. Astonishingly, the band structure of a fully stoichiometric compound appears to be dominated by single-ion crystal-field effects. The large oscillator strength seems to be related with the strong hybridization effects in chalcogenide spinels between the chalcogenide p and the chromium d states.

This work partly was supported by the Deutsche Forschungsgemeinschaft through the German Research Collaboration SFB 484 (University of Augsburg).

Note added in proof

After finalizing this article, evidence was found by synchrotron X-ray diffraction studies that ZnCr_2Se_4 exhibits a lower symmetry than $Fd\bar{3}m$ already in the paramagnetic phase [50]. Thus, the possibility arises that the inversion symmetry at the Cr site is broken, yielding a natural explanation of the huge oscillator strength of the Cr crystal-field excitations.

References

1. T. Rudolf, Ch. Kant, F. Mayr, J. Hemberger, V. Tsurkan, A. Loidl, *New J. Phys.* **9**, 76 (2007)
2. A.N. Yaresko, *Phys. Rev. B* **77**, 115106 (2008)
3. P.K. Baltzer, P.J. Wojtowicz, M. Robbins, E. Lopatin, *Phys. Rev.* **151**, 367 (1966)
4. Y. Yamashita, K. Ueda, *Phys. Rev. Lett.* **85**, 4960 (2000)
5. O. Tchernyshyov, R. Moessner, S.L. Sondhi, *Phys. Rev. Lett.* **88**, 067203 (2002)
6. J. Akimitsu, K. Siratori, G. Shirane, M. Iizumi, T. Watanabe, *J. Phys. Soc. Jpn.* **44**, 172 (1978)
7. M. Hidaka, N. Tokiwa, M. Fujii, S. Watanabe, J. Akimitsu, *Phys. Status Solidi B* **236**, 9 (2003)
8. J. Hemberger, H.-A. Krug von Nidda, V. Tsurkan, A. Loidl, *Phys. Rev. Lett.* **98**, 147203 (2007)
9. H. Murakawa, Y. Onose, K. Ohgushi, S. Ishiwata, Y. Tokura, *J. Phys. Soc. Jpn.* **77**, 043709 (2008)
10. K. Siratori, E. Kita, *J. Phys. Soc. Jpn.* **48**, 1443 (1980)
11. J. Hemberger, T. Rudolf, H.-A. Krug von Nidda, F. Mayr, A. Pimenov, V. Tsurkan, A. Loidl, *Phys. Rev. Lett.* **97**, 087204 (2006)
12. A.B. Sushkov, O. Tchernyshyov, W. Ratcliff, S.-W. Cheong, H.D. Drew, *Phys. Rev. Lett.* **94**, 137202 (2005)
13. R. Valdés Aguilar, A. B. Sushkov, Y. J. Choi, S.-W. Cheong, H.D. Drew, *Phys. Rev. B* **77**, 092412 (2008)
14. T. Rudolf, Ch. Kant, F. Mayr, J. Hemberger, V. Tsurkan, A. Loidl, *Phys. Rev. B* **75**, 052410 (2007)
15. RefFIT by A. Kuzmenko, University of Geneva, Version 1.2.44 (2006), <http://optics.unige.ch/alexey/refit.html>
16. D.L. Rousseau, R.P. Bauman, S.P.S. Porto, *J. Raman Spectrosc.* **10**, 253 (1981)
17. T. Rudolf, Ch. Kant, F. Mayr, J. Hemberger, V. Tsurkan, A. Loidl, *Phys. Rev. B* **76**, 174307 (2007)
18. K. Wakamura, T. Arai, *J. Appl. Phys.* **63**, 5824 (1988); K. Wakamura, T. Arai, *Phase Trans.* **27**, 129 (1990)
19. C.J. Fennie, K.M. Rabe, *Phys. Rev. Lett.* **96**, 205505 (2006)
20. J.M. Wesselinowa, A.T. Apostolov, *J. Phys.: Condens. Matter* **8**, 473 (1996)
21. P.G. Radaelli, *New J. Phys.* **7**, 53 (2005)
22. M. Reehuis, A. Krimmel, N. Büttgen, A. Loidl, A. Prokofiev, *Eur. Phys. J. B* **35**, 311 (2003)
23. M. Hidaka, M. Yoshimura, N. Tokiwa, J. Akimitsu, Y.J. Park, J.H. Park, S.D. Ji, K.B. Lee, *Phys. Status Solidi B* **236**, 570 (2003)
24. V. Tsurkan, J. Hemberger, A. Krimmel, H.-A. Krug von Nidda, P. Lunkenheimer, S. Weber, V. Zestrea, A. Loidl, *Phys. Rev. B* **73**, 224442 (2006)
25. F. Yokaichiya, A. Krimmel, V. Tsurkan, I. Margiolaki, P. Thompson, H.N. Bordallo, A. Buchsteiner, N. Stüßer, D. N. Argyriou, A. Loidl, *Phys. Rev. B* **79**, 064423 (2009)
26. S.-H. Lee, G. Gasparovic, C. Broholm, M. Matsuda, J.-H. Chung, Y.J. Kim, H. Ueda, G. Xu, P. Zschack, K. Kakurai, H. Takagi, W. Ratcliff, T.H. Kim, S.-W. Cheong, *J. Phys.: Condens. Matter* **19**, 145259 (2007)
27. S. Suga, S. Shin, M. Taniguchi, K. Inoue, M. Seki, I. Nakada, S. Shibuya, T. Yamaguchi, *Phys. Rev. B* **25**, 5486 (1982)
28. M. Zvara, V. Prosser, A. Schlegel, P. Wachter, *J. Magn. Magn. Mater.* **12**, 219 (1979)
29. T. Rudolf et al., unpublished
30. G. Busch, B. Magyar, P. Wachter, *Phys. Lett.* **23**, 438 (1966)
31. G. Harbeke, H. Pinch, *Phys. Rev. Lett.* **17**, 1090 (1966)
32. H.W. Lehmann, G. Harbeke, *Phys. Rev. B* **1**, 319 (1970)
33. E. Callen, *Phys. Rev. Lett.* **20**, 1045 (1968)
34. R.M. White, *Phys. Rev. Lett.* **23**, 858 (1969)
35. T. Kambara, Y. Tanabe, *J. Phys. Soc. Jpn.* **28**, 628 (1970)
36. S.B. Berger, L. Ekstrom, *Phys. Rev. Lett.* **23**, 1499 (1969)
37. S. Wittekoek, P.F. Bongers, *Solid State Commun.* **7**, 1719 (1969)
38. G. Harbeke, H.W. Lehmann, *Solid State Commun.* **8**, 1281 (1970)
39. D.L. Wood, J. Ferguson, K. Knox, J.F. Dillon Jr., *J. Chem. Phys.* **39**, 890 (1963)
40. A.D. Liehr, *J. Chem. Phys.* **67**, 1314 (1963)
41. L.L. Golik, Z.É. Kun'kova, T.G. Aminov, G.G. Shabunina, *Phys. Solid State*, **38**, 717 (1996)

- 42. P.K. Larsen, S. Wittekoek, Phys. Rev. Lett. **29**, 1597 (1972)
- 43. D.L. Wood, G.F. Imbusch, R.M. Macfarlane, P. Kisliuk, D.M. Larkin, J. Chem. Phys. **48**, 5255 (1968)
- 44. S. Sugano, Y. Tanabe, H. Kamimura, *Multiplets of Transition-Metal Ions in Crystals* (Academic Press, New York, 1970)
- 45. J. Deisenhofer, I. Leonov, M.V. Eremin, Ch. Kant, P. Ghigna, F. Mayr, V.V. Iglamov, V.I. Anisimov, D. van der Marel, Phys. Rev. Lett. **101**, 157406 (2008)
- 46. H. Szymczak, W. Wardzyński, A. Pajęczkowska, J. Magn. Magn. Mater. **15-18**, 841 (1980)
- 47. Ch. Kant et al., unpublished
- 48. M. Taniguchi, A. Fujimori, S. Suga, Solid State Commun. **70**, 191 (1989)
- 49. K. Ohgushi, Y. Okimoto, T. Ogasawara, S. Miyasaka, Y. Tokura, J. Phys. Soc. Jpn. **77**, 034713 (2008)
- 50. A. Krimmel, private communication